Solid Freeform Fabrication 2024: Proceedings of the 35th Annual International
Solid Freeform Fabrication Symposium – An Additive Manufacturing Conference
Reviewed Paper

# A Design and Additive Manufacturing Framework for Voxel-Based, Multi-Material, Thick-Folding Origami

**Evelyn Thomas [1], Jared Butler [2], Nicholas Meisel *[2]**
* Corresponding Author: nam20@psu.edu
[1] Department of Mechanical Engineering, The Pennsylvania State University, University Park, PA 16802
[2] School of Engineering Design and Innovation, The Pennsylvania State University, University Park, PA 16802

## Abstract

Origami has expanded beyond its paper-craft origins to solve problems related to volumetric constraints and deployment within fields such as aerospace engineering, civil engineering, and biomedical engineering. While paper folding enables the design of complex mechanical systems that can inspire engineering designs, realizing these systems in thick, engineered materials requires additional design and manufacturing considerations when contrasted against traditional, thin origami. Methods to accommodate for thickness in origami-based systems require numerous processes and assembly steps. However, the material and functional complexity of voxel-based additive manufacturing can address the drawbacks inherent to traditional thick-folding origami. Design at the voxel level can allow for precise and continuous functionally graded material properties that enable novel behavior and improve the overall performance of thick-folding origami designs. This paper details a framework for designing voxel-based additive-manufactured thick-folding origami parts. This framework is demonstrated through two case studies that show the application of voxel-based multi-material additive manufacturing to thick-folding origami techniques.

## 1. Introduction

Origami is a paper art form based on a zero-thickness model. Origami-based design [1] has been applied to engineering applications where volume reduction or motion is essential. As an example, Edmonson et al. developed an origami-adapted forceps [2] for robotic surgeries. Unlike traditional forceps, the "Oriceps" can flatten, thus reducing its bounding volume. This is useful in minimally invasive surgery given the typical restriction on space. Similarly, Butler et.al. used Kapton to manufacture compressible bellows [3]. The kinematics of the bellows was based on the Kresling origami pattern [3]. This design is ideal for environments such as outer space, where volume minimization is necessary. Additionally, the mathematical principles involved in folding origami have been applied to robotic design [4]. The folding contributes to the robot's assembly [5], motion [6], and ability to interact with its environment [7].

While such origami-based designs have solved engineering problems, they are limited to the use of thin materials because the mathematical relationships within origami are based on thinness. Most engineering materials have considerable thicknesses that must be accounted for when origami-based designs are used. Thick-folding Accommodation Methods (TAMs) have been de-

veloped to introduce origami-based design principles to traditionally thick engineered materials [8–11]. These thick-folding methods can preserve the desirable behaviors present in thin origami designs while translating them for use in thicker materials. Unfortunately, TAMs often require a greater number of processes and assembled sub-parts compared to additively manufactured parts. The added complexity, labor, and time needed to manufacture a TAM may make them unrealistic for large-scale use.

Given the challenges associated with TAMs, there is the possibility to leverage additive manufacturing to reduce part count and assembly time while providing unique opportunities for complexity. Multi-material additive manufacturing (MMAM), in particular, enables the manufacturing of parts that contain regions of varied elastic moduli, creating functional opportunities without requiring assembly. Multi-material AM mechanisms have been produced [12] using discrete [7] and functionally-graded [13] material design methods.

Functionally-graded structures could prove especially promising to the design of thick-fold origami, due to the ability to tailor material properties throughout a continuum in 3D space. Functionally-graded parts are designed using voxels, volumetric representations of pixels. Material properties can be assigned to each voxel in a discretized or continuous gradient [14]. In this way, voxel-based design, when used in conjunction with AM, may be utilized to address the manufacturing and assembly challenges typically associated with thick-folding origami-based parts. Flexible and rigid elements can be produced in one process, with parts designed as a singular body and assigned material attributes at the voxel level. In this way, voxel-based gradients may even help to reduce failure at the interfaces of dissimilar material properties [14].

Merging origami-based thick-folding mechanisms, additive manufacturing, and voxel-based design will create new engineering design possibilities that are more robust and efficient to manufacture. However, a framework is needed to assist engineering designers in navigating the complexities that arise from interdisciplinary design. The elements of opportunistic additive manufacturing that enable these mechanisms must be balanced by restrictive additive manufacturing. Meanwhile, the kinematic properties of the TAMs must still be preserved. In some cases, geometric modifications must be made to create printable parts. As a result of this need, this paper provides a framework for selecting a TAM as well as the design and manufacturing considerations needed to successfully additively manufacture a multi-material thick-folding origami-based part.

## 2. Background

The ability to design voxel-based, thick-folding origami parts relies on understanding the mathematical bases of origami, how these bases apply to origami, and how additive manufacturing has been used to produce origami-based designs previously. With this information in mind, voxel-based design can be applied to origami-based designs.

### 2.1. Theories of Origami-based Engineering Design: Zero-thickness Model & Thick-Folding

Traditional thin-folding origami is based on the zero-thickness model (ZTM) [15], which represents a theoretical possibility where thickness does not impact folding. This model is shown in Figure 1 using the zero-thickness line. While the origami-based structure is folded, the zero-

thickness line would coincide with itself. The ZTM can be used as a model for examining motion and kinematics relative to the theoretical case [15]. One of the closest real-world examples to this ideal case is printer paper. Printer paper is about 0.11 mm thick [16], which is at least an order of magnitude thinner than most thick-folding origami. The thinness of the printer paper means any straining or interference is negligible when compared to thick-folding origami. As thickness increases, deviation from the zero-thickness model increases, which leads to interference and/or resistance to folding. As a result, thickness accommodation methods (TAMs) were needed to account for the excess material.

Thickness accommodation methods have been developed to reduce or remove interference while retaining many of the characteristics of thin-folding origami, as shown in Figure 1. These methods maintain basic origami characteristics such as non-folding regions (panels) and the ability to fold up (mountain fold), or down (valley folds). The scope of the work presented in this paper centers on two types of origami mechanisms: planar mechanisms and spherical mechanisms. Planar mechanisms are designed for two-dimensional motion [17], spherical mechanisms (simple spatial mechanisms [18]) move in three dimensions [17] . Unlike spatial mechanisms, planar mechanisms have pleat-like folds that remain planar when folded [19]. For spherical mechanisms, the axes of revolutions, or fold lines, all point towards a point [20]. As such, the "line of zero-thickness" for spherical mechanisms is actually a plane.

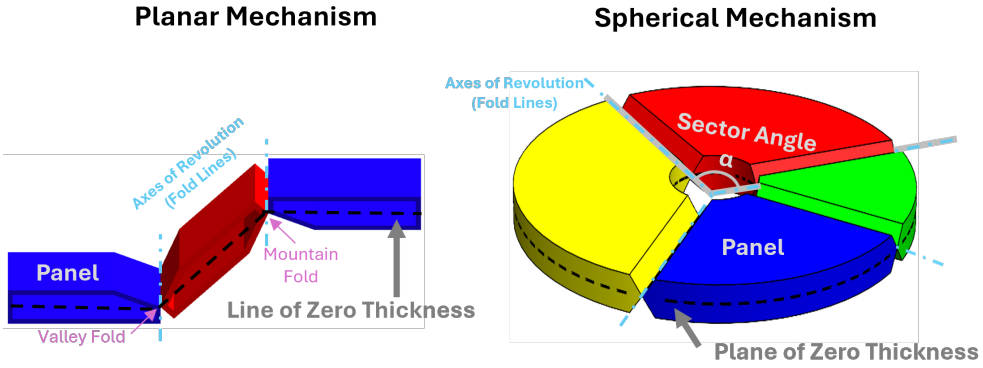


**Figure 1:** Planar Mechanism vs. Spherical Mechanisms

TAMs preserve the motion and/or kinematics of the zero-thickness model in different ways [15]. Typically, this involves shifting the axes of rotation, removing material, or adding strain elements. As an example, in their Eggbox tessellation, Yellowhorse et al. [21] shifted the axes of rotation to the edges of the panels and connected the panels using tape. Shimoda et al. used the same method but connected the panels using hinges [22]. Tachi et. al. removed material to accommodate thickness with the layered tapered panels method. In one of their pieces, applied this method using 2-ply double-walled cardboard adhered to cloth [23]. Butler et al. added a flexible sheet of spring steel bolted between acrylic panels [10]. The strain energy of flexible materials allows parts to bend and accommodate more thickness. While all of these examples utilize thickness accommodation methods to accomplish their goals, these parts were made using subtractive manufacturing and required assembly. Additionally, other parts such as bolts, rivets, pins, stock hinges, and adhesives are commonly used to assemble thick-folding origami. Additive

manufacturing can reduce the number of parts and processes associated with producing thick-folding origami.

### 2.2. Additive Manufactured Origami

Additive manufacturing has previously been used to produce thick-folding origami, though in a limited capacity. Single-material examples include using lamina emergent torsional joints or strain joints to achieve a 3D shape from a planar print [24, 25]. Kim et al. used additive manufacturing for the panels and latex and nylon bands [26] for a rolling contact joint prosthetic hand. Similarly, Boisclair et al. additively manufactured their prosthetic hand prototype using resin and cords [27]. In these examples, the panels are additively manufactured, but pins [28] or tape [29] are used to achieve the motion. Because of this, although AM is used to create these designs, they do not fully take advantage of AM's design opportunities such as geometric, functional, and material complexity. However, fully additively manufactured functional parts can be realized using multi-material AM.

Strain-based multi-material origami-based mechanisms have been manufactured using AM; however, they are limited by restrictive AM. Lee et al. created a twisting mechanism based on the Kresling pattern using material jetting [30]. Stankovic et al. stacked a square twist origami pattern using material jetting [31]. MMAM has been used to improve hand orthoses [32] using a strain joint and a spring origami gripper [33] has been created using a membrane fold. While all of these examples are fully additively manufactured parts, they do not address some of the more restrictive elements of AM such as premature yielding due to anisotropy. MMAM makes origami-based design more efficient, though delamination and excess stress between material phase are concerns. Origami-based systems rely on large deflections, which lead to high stresses and strains. Researchers such as Ye et al. [34] have been working to make these MMAM systems more reliable. Their method for creating self-locking thick panel origami involved fully enveloping the rigid panel within the flexible material so the outer layers of the part were comprised of the same material [34]. Wagner et al. and Delimont et al. have used reduced area joints [35], or cutouts [36], to reduce stress. Hunter et al. have experimented with printing multi-material hinges with cutouts of different shapes [37]. Gradients can also reduce the likelihood of failure by delamination caused by improper bonding of dissimilar materials [14]. MMAM origami-based designs will be improved by leveraging voxel-based gradients and other stress mitigation design strategies.

The multi-material AM origami-based parts have increasingly improved the efficiency of origami-based designs. Adding voxel-based gradients will further improve this by reducing the likelihood of failure. In light of this existing body of research, there exists a need to better understand how the thick-folding origami-based parts may be produced using voxel-based design. To address this, the remaining sections of this paper will provide a framework to design and manufacture a thick-folding multi-material additively manufactured origami-based part using voxel-based design.

## 3. Design & Manufacturing Considerations Framework

To address the research opportunity from Section 2, we propose a two-tiered framework meant to assist designers with (1) identifying and selecting an AM-relevant TAM and (2) specifying

key design and manufacturing guidelines associated with voxel-based MMAM in thick-folding origami-based parts.

Prior to using the provided design guidelines, the user must select a TAM. The framework in this paper provides a method to help the user select one of the seven TAMs [15]. These TAMs are shown in Figure 2. Initial down-selection is essential for properly implementing the design and manufacturing guidelines provided later. If the user already has a TAM in mind, they can proceed to Section 3.2. If not, the user may select one based on the fundamental relevance of the different TAM approaches to AM in Section 3.1. After selecting a TAM, this framework provides design and manufacturing guidelines for producing thick-folding origami with voxel-based design for Additive Manufacturing. These considerations covered include geometry, material, and printing considerations.

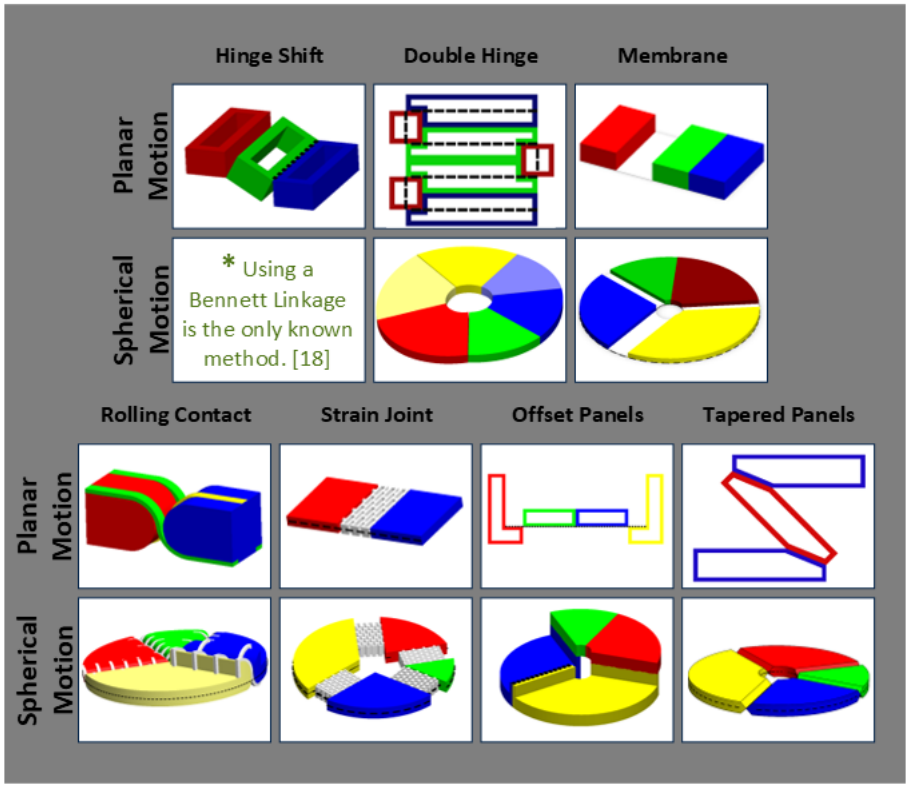


**Figure 2:** The seven TAMs covered in this paper as planar and spherical mechanisms are shown here.[15]

### 3.1. Selection of Thick-Folding Origami Designs for AM

The authors propose an Additive Manufacturing Opportunity Score, which can help identify the TAMs with the greatest likelihood to act as a functional showcase for AM. A higher Additive Manufacturing Opportunity (AMO) Score correlates to a TAM that would greatly benefit from AM adoption over traditional manufacturing methods. A lower AMO Score indicates the TAM is already suitable for AM, with few, if any, modifications. The AMO Score is based on Lang, et al.'s estimation of the minimum number of processes and part count to use each TAM [15]. For the purposes of this paper, "part" refers to a complete entity, while "subparts" refer to individual

parts that can be assembled into a part. As a result, the part count mentioned in the Lang et al. publication is equivalent to a subpart in this paper.

The inputs for the AMO Score can be found in Table 1. It is important to note that some of the methods include designations such as "monolithic" or "layered." These are based on the constraints imposed by traditional means of construction. When constructing these methods using AM, these designations will not exist, based on AM's ability to create geometries of seemingly infinite complexity without added manufacturing cost.

| Thickness Accommodation Method | Min. # Processes | Sub-part Count (Score) | AMO Score |
|---|---|---|---|
| Strain Joint | 1 | Low (1) | 0 |
| Membrane | 2 | Low (1) - Baseline (2) | 1 - 3 |
| Integrated Rolling Contact Joint | 3 | Low (1) | 2 |
| Layered Tapered Panels | 2 | High (3) | 5 |
| Monolithic Hinge Shift | 3 | Baseline (2) | 5 |
| Monolithic Offset Panels | 3 | Baseline (2) | 5 |
| Monolithic Tapered Panels | 3 | Baseline (2) | 5 |
| Separate Rolling Contact Joints | 3 | Baseline (2) | 5 |
| Layered Hinge Shift | 2 | High (3) - V. High (4) | 5 - 7 |
| Segmented Offset Panel | 2 | High (3) - V. High (4) | 5 - 7 |
| Layered Double Hinge | 2 | High (3) - V. High (4) | 5 - 7 |
| Monolithic Double Hinge | 3 | High (3) | 8 |

**Table 1:** Additive Manufacturing Opportunity (AMO) Score Based on Values Found in [15]

The minimum number of processes ranged from 1 to 3. The sub-part count scores were assigned as follows: "Low" = 1, "Baseline" = 2, "High" = 3, and "Very High" = 4. The AMO Score was calculated by multiplying the sub-part category score by the minimum number of processes and subtracting one (the lowest possible score for a fully additively manufactured part). Once adapted for AM, the complexity score for fully additively manufactured parts would be "0" for six of the seven methods because MMAM allows for most parts to be produced as a single-process assembly. The score for the AM-adapted Rolling Contact Joint would be "1"; the strain is obtained by stretching the flexures that must be printed straight, then curved and secured in place [38]. Based on the values presented in Table 1, a user might note that a fully additively manufactured strain joint provides no benefit over subtractive manufacturing, as the current process for making this is already well-suited for AM. By contrast, the complexity of the double hinge TAM would make it the ideal candidate for AM adoption due to the high sub-part count and number of processes needed for production.

### 3.2. Accounting for DfAM in Thick-Folding Origami-based Joints

This section walks the user through Figure 3, which focuses on the portion of the framework that provides the design and manufacturing variables needed to successfully produce the TAM chosen in Section 3.1. There are three major design variable categories for creating MMAM thick-folding origami: geometric, material, and printing considerations. Some variables (shown in blue) on Figure 3 are situational and need to be user-defined. Items in grey are hard restrictions and/or

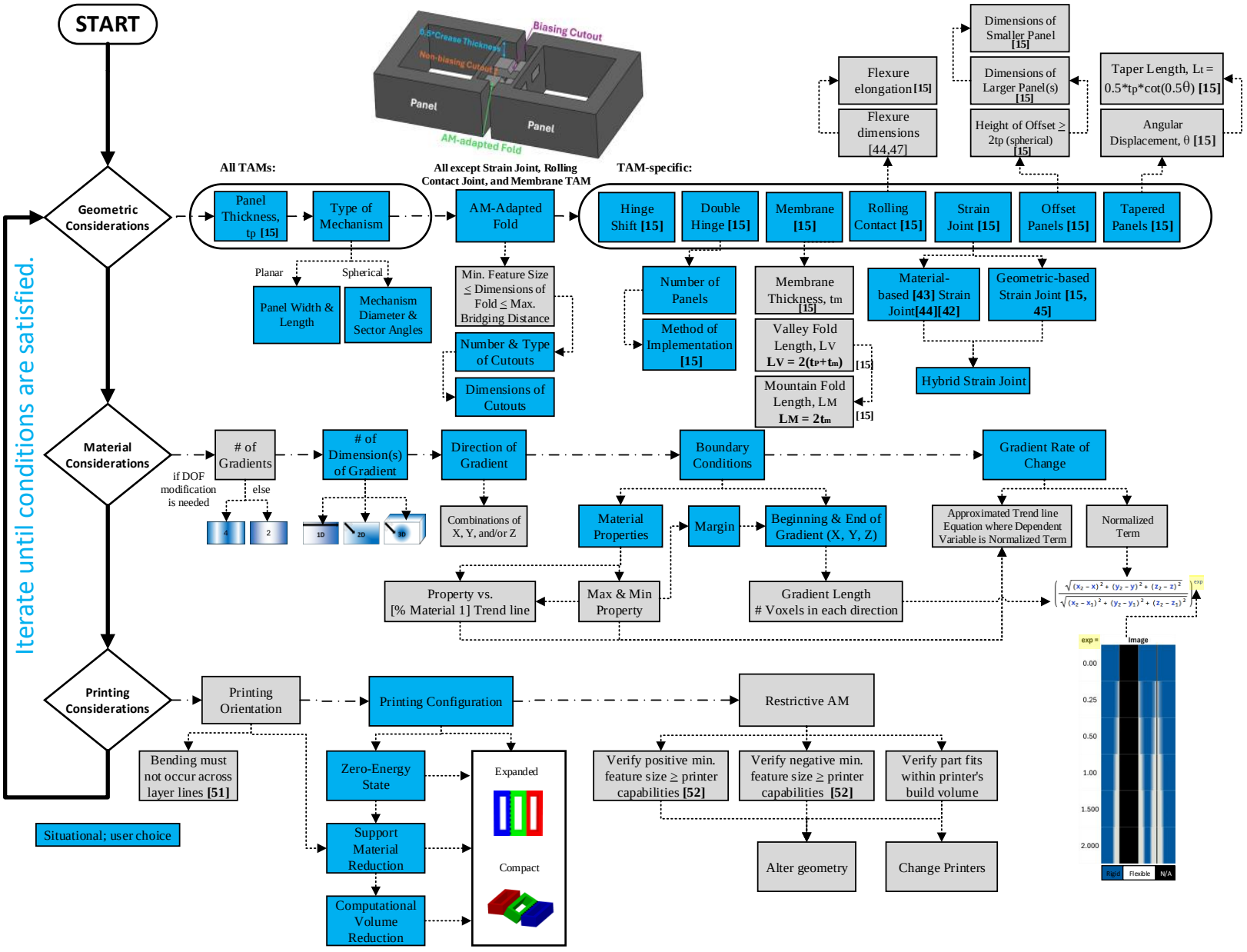


**Figure 3:** This framework provides guidance for designing and manufacturing multi-material ad-ditively manufactured thick-folding origami.

governed by formulae. The user may need to iterate through the framework if printing considerations are invalidated.

### 3.2.1 Geometry

Geometry is the first of the three consideration categories. To begin with, the framework has the user select a panel thickness and the type of mechanism (planar or spherical) as shown in Figure 3. The panel thickness is the most important dimension for the user to define, as several formulas used later rely on this value. The mechanism type determines the panel's other geometric variables. Another important dimension for spherical mechanisms is the sector angles. Sector angles refer to the angle between the radii that bound each panel, as shown in Figure 1. Selecting angles and their proximity to one another will influence the motion of the design; mathematical relationships govern properties such as flat-foldability [15][22].

Next, the framework introduces the idea of an AM-adapted fold, which occurs at a vertex where minimizing material is prioritized. Typically, these panels would be attached using an adhesive or pin; however, a fully-compliant, additively manufactured solution is to create a minimally-active fold. An example of this is in Figure 3. This is only necessary for methods that are not easily adapted for AM, therefore it excludes the membrane, rolling contact joint, and strain joint TAMs. This AM-adapted fold is required for TAMs that need a minimum distance between parts to prevent the panels from fusing during printing. This distance should be minimized as much as possible to retain the intended motion of TAM. Methods with geometries that can easily be adapted for MMAM, such as the strain joint, rolling contact joint, and membrane TAM can use a flexible material where bending must occur [39, 40]. The dimensions of the fold are subject to the minimum feature size and the bridging distance of the printer. The AM-adapted folds can take many forms. The example provided in the framework depicts one non-biasing cutout and two biasing cutouts. Cutouts may be used to reduce stress [41] or to bias the material to bend in a certain direction by taking the second moment of the area into account. Triangular or "notch"-style cutouts can ensure the design is more likely to bend in one direction. These are biasing cutouts. Non-biasing cutouts may also be needed to reduce the stress [41].

The rest of the geometric considerations are TAM-specific. The user should proceed with the TAM chosen in Section 3. The relevant points of concern, as they relate to AM, are summarized in this subsection. The Hinge Shift TAM will not be elaborated upon because the design variables have been previously covered in this section. Additionally, the Double Hinge TAM will not be discussed in further detail because this TAM can be implemented in several ways[15]. Broadly speaking, in addition to the method of implementation, the number of panels (links in the Gruebler equation [18]) must be determined. Similarly, the Strain Joint TAM can be produced in many ways, geometry-based, material-based, or a combination of the two (hybrid). The geometric-based methods are those that primarily use geometry to obtain motion. Typically, this involves using a type of torsional joint acting as a surrogate fold [40], such as a Lamina Emergent Torsional (LET) Joint [15][42]. Material-based methods rely upon materials[34] with low Young's modulus and high Poisson's ratio[43] that can stretch to accommodate thickness. These methods can also be combined into a hybrid approach, such as a Membrane-enhanced LET Joint [44]. Due to the variety of methods that can be employed, further design variables will not be provided here.

The Membrane TAM uses thick panels atop a thin membrane. As discussed in Section 3.1, this method has different requirements for mountain and valley folds. The mountain fold length is found in Equation 2, where $L$ refers to the length, $t$ refers to the thickness, and the superscripts $m$ refers to the membrane, and $M$ refers to the mountain fold.

$$L_M = 2t_m \tag{1}$$

In traditional manufacturing, panels undergoing a mountain fold abut each other because the membranes used in these methods approximate zero-thickness and negligible strain [10]. Additively manufactured membranes must be thicker than traditional membranes due to the conditions imposed by minimum feature size. Given that strain is approximately negligible based on the definition of the membrane [10] TAM, the mountain fold length is twice the thickness of the membrane.

$$L_V = 2(t_P + t_m) \tag{2}$$

The valley fold length is governed by Equation 2, which uses the same variables in the previous equation but also includes $P$ to refer to panels, and $V$ to refer to the valley fold. The length of the valley fold is much larger than the mountain fold because must account for folding over one of the panels. As a result, the panels must be spaced no less than twice the panel and membrane thicknesses apart. If this distance was made smaller, there would be unnecessarily high strain caused by the membrane stretching to reach this distance, leading to premature failure.

The Rolling Contact Joint TAM can be produced in many ways, including a tension-based CAM system called COmpliant Rolling-contact Elements (CORE) [38] and Synchronized-offset-rolling-contact element (SORCE) [45]. Both methods require flexures that will strain to allow motion, as well as a small gap between panels. The diameter of the curved regions is equivalent to the panel thickness. For a flat-foldable model spherical mechanism, the rolling contact joints adjacent to the largest two panels must be raised by the panel thickness; the total height for this section will be twice the panel thickness, assuming all panels have the same thickness [45]. The elongation of the flexures is based on the dimensions of the flexures and their material properties.

The Offset Panels TAM is ideal for creating thick-folding origami that sandwiches together neatly. Interference is avoided by removing material from two panels (typically the largest) and adjusting the position of the other two panels. Moving the uncut panels so that the hinge is aligned with the cut edges of the other two panels preserves the zero-thickness line. The length and width of the removed region should be equivalent to the dimension of the panel abutting it. For spherical mechanisms using this method, the height of the offset must be equal to the panel thickness to prevent interference. When the lofted panels are placed on top of the larger panels, the unfolded mechanism height should be twice the panel thickness.

The Tapered Panels TAM involves removing material to preserve the zero-thickness model. The angular displacement of the part is essential to determining how much material should be removed. A higher angular displacement and thickness yields a longer taper. The formula for the taper can be found in Figure 3 and Equation 3,

$$Taper\ Length = \frac{t_P cot(\frac{\theta}{2})}{2} [15] \tag{3}$$

where $\theta$ is the angular displacement.

### 3.2.2 Material Considerations

The next category of considerations found on the framework in Figure 3 is based on materials. The type of materials used and their method of application can change the motion of thick-folding origami. A gradient between flexible and rigid materials can act as a pseudo hinge when applied to a TAM. In this paper, a gradient is defined as a transition from one property to another. In MMAM, gradients allow the part to transition from a primarily rigid to a primarily flexible base material, which can enable bending without the need for abrupt material property transitions. The number of gradients is usually two for most bending applications (rigid-to-flexible, flexible-to-rigid); however, using four gradients can add a new rigid link. This new link modifies Gruebler's equation [18]. The added degrees of freedom (DOF) can rectify an over-constrained system[45][46].

After the number of gradients is determined, each gradient must be assigned a number of dimensions and direction(s). The number of dimensions refers to the way the gradient varies within space, as shown in Figure 3. A one-dimensional (1D) gradient occurs in a straight line along the X, Y, or Z direction. Two-dimensional (2D) gradient would be a radial or diagonal gradient that occurs in two directions. A three-dimensional (3D) gradient would look like a graded geometric solid or lattice [47]. It is recommended to select the lowest dimension that meets the needs of the parts. Oftentimes, a 1-D gradient is sufficient; however, higher-order dimensions may be needed to properly constrain rigidity in the part. This will be discussed in greater detail in Section 4.

Next, in Figure 3 are the boundary conditions. Boundary conditions are governed by the material properties and the beginning and end of each gradient. In many cases, the material property gradient [48] and color gradient are not linear [14]. The vast difference in properties between a highly rigid and highly flexible material typically means gradients in a 1:1 (rigid:flexible) volumetric ratio may still be very rigid, compared to a fully flexible region. Depending on the design and the materials available, the user may wish to start with a maximum property less than the most rigid material available or a minimum property greater than the most flexible material available. For example, 80% rigid maximum property and 90% flexible minimum property instead of 100% of both. A relationship between the property of interest (dependent variable) and the ratio of the materials will assist in determining the location of the most flexible and rigid regions. Most trend line equations are designed to reduce the average error, which means they often do not perfectly align with the first and last point. It may be necessary to adapt this trendline to ensure the boundary conditions of the minimum and maximum property values are maintained. Efforts should be made to preserve the order of magnitudes within the equations when constructing the approximate trend

line equation. An example can be found in Equation 4

$$Property(N) = AN^3 + BN^2 + CN + [Min.Property],$$
where Property = Minimum Property when N = 0 & Property = Maximum Property when N = 1 (4)

where $N$ is a Normalization Term that is explained later, and $A$, $B$, and $C$ are coefficients in the approximate trend line equation. It is noteworthy to clarify that gradients are purely focused on transitions; however, in some cases, it may be necessary to have regions that remain fully flexible or fully rigid for longer than one voxel, especially when the area in which the folding occurs is small. It is often helpful to include a margin that extends these regions to decrease the likelihood of stress concentrations [49, 50] at the locations of the most flexible regions. Increasing the margin too much would shorten the amount of space available for the gradient length.

The beginning and end of each gradient in each Cartesian direction must be established by the user. This is based on the areas of high flexibility or rigidity as well as the margin. When subtracted, this is the gradient length, which is the number of voxels in each direction. A longer gradient provides greater support for thin regions because the material becomes dissimilar more slowly. This will, in turn, decrease stress concentrations [49, 50]. When placing the gradient on the TAM, it may seem as though the gradient should only traverse folds; however, maximum material flexibility must occur where maximum bending is meant to occur; this is typically at the middle of the AM-adapted fold or the edge of the panels for the membrane TAM. The gradients must start within the panels to ensure full flexibility where maximum bending occurs while preventing sharp gradients. Generally, panels are thicker than most flexible regions; even at the same Young's Modulus, panels will resist bending more than AM-adapted folds or membranes, due to the higher second moment of the area. As a result, the increasing flexibility in the panels will not change where bending occurs.

The gradient rate of change is the rate at which the gradient transitions from one property to another. The trend line discussed earlier in this section provides a relationship between concentration and properties; however, it is necessary to normalize the distance in each gradient direction. The boundary conditions provided are inputs into the Normalized Term in Equation 5,

$$N(x,y,z) = \left( \frac{\sqrt{(x_2-x)^2 + (y_2-y)^2 + (z_2-z)^2}}{\sqrt{(x_2-x_1)^2 + (y_2-y_1)^2 + (z_2-z_1)^2}} \right)^{exp} \tag{5}$$

where the letters "x", "y", and "z" are the directions, the subscript "1" represents the smallest voxel in gradient, and the subscript "2" represents the largest voxel in the gradient. The "exp" term is an exponent that governs the how quickly the gradient transitions from the maximum property to the minimum property; the larger the number, the greater the spread. This must not be confused with any exponents already in the approximate trendline equation, shown in Equation 4. Figure 3 shows a comparison of how this term impacts the rate of the gradient. This equation identifies the distance in each of the directions used relative to the maximum distance possible. For this reason, any unused dimensions should be removed from the equation. The Normalized Term will produce a value from 0 to 1, which will be used inside the material property trend line equation, in place of the dependent variable. The STL file containing the geometry of the part, boundary conditions,

and the equations concerning the gradient can be input into MATLAB for voxelization, dithering, and slicing.

Once the material conditions governing the design have been set, the printing considerations are established.

### 3.2.3 Printing Considerations

There are three main printing considerations: printing orientation, printing configuration, and restrictive AM.

Printing orientation is the way the part is arranged on the build plate. For functional parts such as origami-based systems, emphasis is placed on part function, as opposed to time and support material reduction. Due to the anisotropy of additive manufacturing, parts are weakest when loaded perpendicular to the build direction [51]. For bending moments, this correlates to rotating about the layer lines; parts should be printed to avoid this.

The printing configuration is the as-printed state of the part before bending. The expanded form will take up more space on the build plate as compared to the compact form. Printing in either the fully expanded or fully compact form may not be possible due to fusing. As a result, the compact form will represent the most compact geometry that can be achieved without fusing and the expanded form will represent the most expanded geometry that can be achieved without fusing. The distance between panels must be greater than or equal to the minimum feature size is preserved throughout the part. There are three main things to consider when deciding the printing configuration: the zero-energy state, support material, and computational volume. The first and most important is a functional variable: the zero-energy state. The zero-energy state is the default configuration of the origami-based part without actuation. If this origami-based part is expected to be expanded in its default shape, it is recommended to print in the expanded configuration. If the part is folded and unfolded repeatedly, this consideration is less impactful. The user may consider the impact of reducing support material and computational expense. Assuming the ideal printing orientation is used, support material is not a concern for most planar mechanisms printed in the expanded configuration. The rolling contact joint TAM is an exception because of the flexures that must be printed straight. The AM-adapted fold links panels that are very close together. This small distance allows bridging to occur, thus eliminating the need for support material. The sophisticated motion of the spherical mechanisms will often require more support material if printed in the compact configuration, as opposed to the expanded configuration. Note that this framework aims to be process-agnostic, therefore; support material is mentioned. If processes such as binder jetting or laser powder bed fusion of polymers are used, this concern will not be relevant. Finally, the computational expense is an important concern. The voxelization process in MATLAB is based on the computational volume. This is the total number of voxels in the X, Y, and Z dimensions multiplied by each other. This is not equivalent to the part volume. For example, when using the Membrane TAM, the difference in the membrane thickness and the panel thickness causes the actual part volume to differ from the voxelized volume. The subtracted material must still be processed computationally and, thus, increases the computation time as well as the computational requirements. As a result, printing compact is often the most efficient configuration. One excep-

tion is printing a compact hinge shift; the spacing needed to prevent fusing slightly increases the computational volume. The positive and negative attributes of both printing configurations must be weighed within the context of the origami-based part's function and the computation resources available.

Lastly, restrictive AM must be evaluated to ensure the part will print successfully. The positive minimum feature size is the minimum amount of material the printer and material can produce. If features that are too fine are attempted, it can lead to missing or incomplete features. The negative minimum feature size is the space between distinct sub-parts. If the spacing left is too small, fusing will occur. This fusing will prevent the part from moving as designed. If fine features or spacing are too small, scaling the part in a proprietary slicer might be a good solution. Unfortunately, scaling the part to make these features printable may cause the part to exceed the printer's build volume. As a result, the part must be checked for printing constraints prior to manufacture. If the printer cannot be changed, the geometry must be altered to prevent printing defects.

Changing design variables based on restrictive AM may alter dependent variables, such as geometry. As a result, it is recommended to iterate through the framework until the printing considerations are satisfied.

## 4. Case Studies

To demonstrate the use of the framework detailed in Section 3, two case studies are presented. In these case studies, the design of the membrane and offset panels planar TAMs were designed using the framework. These TAMs were chosen because they are on the low and medium-high end of the AM Opportunity Table, found in Section 3.1. Note that the scope of the examples in this paper is limited to planar mechanisms and color-based gradient was chosen for illustrative purposes.

### 4.1. Membrane TAM

#### 4.1.1 Geometric Considerations of Membrane TAM

The membrane TAM is one of the most natural panels for initial MMAM adoption as it requires no modification. The planar membrane TAM only requires panel thickness, membrane thickness, mountain fold lengths, and valley fold lengths. The dimensions (in mm) of the planar membrane TAM are shown in Table 2 with annotations in Figure 4. The black represents the flexible membrane and the white represents rigid panels.

The voxelized model shown in Figure 4 was produced using the framework in Section 3.2, starting with geometric considerations. First, the panel thickness (12.5 mm) was chosen to ensure the effects of thick-folding (as opposed to near-zero-thickness folding) would be seen in the final design. As previously stated, the part would use a planar mechanism, which requires the width and length of panels. Given that this part was designed for demonstrative purposes, the remainder of the variables were chosen somewhat arbitrarily while keeping in mind future restrictive AM concepts. Following along on the framework, the AM-adapted Fold section was skipped because it is not required for this TAM. For the TAM-specific geometric considerations, the membrane thickness

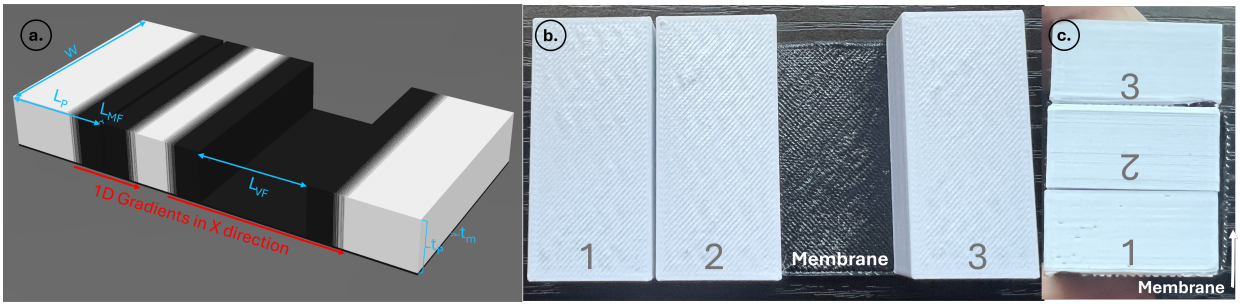


**Figure 4:** Case Study 1: The Membrane TAM. Black represents flexible material and white represents rigid material. (a) Voxel-based design (b) Unfolded Planar Model (MEX) (c) Folded Planar Model (MEX)

| Dimension | Dimension Abbreviation | Value (mm) |
|---|---|---|
| Panel Length | $L_P$ | 25 mm |
| Total Length | L =$L_m$ | 102 mm |
| Valley Fold Length | $L_{VF} = 2t_m$ | 1 mm |
| Mountain Fold Length | $L_{MF} = 2t_P + 2t_m$ | 26 mm |
| Total Width | w = $w_P = w_m$ | 50 mm |
| Panel Thickness | $t_P$ | 12.5 mm |
| Membrane Thickness | $t_m$ | 0.5 mm |
| Total Thickness | t | 13 mm |

**Table 2:** Dimensions used in Case Study 1

(0.5 mm) was chosen before the other key dimensions, due to its impact on other formulae. The total length of the part (102 mm) was based on the length of the panels, the valley fold length from Equation 1, and the mountain fold from Equation 2, as shown in Figure 3. The function of the mechanism as it relates to geometric considerations in the framework was validated using the printed sample in Figure 4 b and c.

### 4.1.2 Material Considerations of Membrane TAM

After the geometry was validated, the material considerations were determined. First, two gradients were used because this TAM did not require DOF modification. Next, a 1D gradient in the "X" direction similar to that shown in Figure 3 was chosen. As stated in Section 3.2.2, it is best to choose the simplest gradient that can accomplish the task. In this case, the membrane is monolithic and the higher second moment of the area of the panels will not allow the panels to bend. This means the panels will not need to be graded in the "Y" or "Z" dimension to prevent bending in undesirable directions.

The boundary conditions were determined by the material properties, margin, and gradient positions. The voxel-based designed part was created to demonstrate the functionality framework. As a result, the authors chose to use a linear relationship between the theoretical materials' concentrations and properties for the approximated trend line. As such, the property remains in variable form. The authors chose to use the full range of material properties to provide a gradient from min-

| Region | Property Status | Start (vx) | End (vx) |
|---|---|---|---|
| Panel 1 | Rigid | 0 | 178 |
| Panel 1 to Long membrane | Rigid to Flexible | 179 | 291 |
| End of Panel 1 +/- 3 | Flexible | 292 | 298 |
| Long Membrane | Flexible to Rigid | 299 | 411 |
| Middle of Long Membrane | Rigid | 412 | 486 |
| Long Membrane to Panel 2 | Rigid to Flexible | 487 | 599 |
| Start of Panel 2 +/- 3 | Flexible | 600 | 606 |
| Panel 2 | Flexible to Rigid | 607 | 719 |
| Panel 2 | Rigid | 720 | 781 |
| Panel 2 | Rigid to Flexible | 782 | 894 |
| Short Membrane | Flexible | 895 | 913 |
| Short Membrane to Panel 3 | Flexible to Rigid | 914 | 1026 |
| Panel 3 | Rigid | 1027 | 1204 |

**Table 3:** Boundary Conditions for Membrane TAM

imum property (0) to maximum property (1). Next, a margin of $\pm$ 3 voxels was used to increase the size of the fully-flexible (minimum property) region. This value was chosen to be sufficient based on geometric constraints. An odd margin number was chosen to ensure symmetry about the minimum property region. A $\pm$1 voxel margin proved insignificantly small; whereas a $\pm$5 voxel margin would significantly decrease the gradient length for the shorter membrane. The first gradient began 60% into the total length of the first panel. This value was chosen ensure the gradient length would be significant while retaining maximum rigidity for over half of the panel. This value is specific to the geometry included in this case study. Once the boundary conditions, shown in Table 3 were determined, the gradient rate of change equation was assembled.

When applied to Equation 4, combined with Equation 5, and simplified for a 1D gradient, the gradient rate of change is

$$Property(x) = \left( \frac{\sqrt{(x_2 - x)^2}}{\sqrt{(x_2 - x_1)^2}} \right)^{exp} + [Min.Property] \tag{6}$$

where Property = Minimum Property when x = $x_2$ & Property = Max. Property when x = $|x_2 - x_1|$. The exponent ("exp") on the normalization term was set to "2" to produce a more drastic gradient than a fully linear relationship would create, for demonstrative purposes.

### 4.1.3 Printing Considerations of Membrane TAM

This part was in the XY orientation for two reasons. First, printing in this configuration would ensure bending would not occur across layer lines. Secondly, this orientation is the best orientation for reducing support material, partially based on the printing configuration. The printing configuration has three major considerations: zero-energy state, support material, and computational volume. This part was designed for demonstrative purposes, therefore the zero-energy state requirement was irrelevant. Printing in the expanded configuration would reduce support material; therefore, the expanded configuration was used. As mentioned in Section 3.2.3, this configuration

has a higher computational load for this TAM. As such, if the computational volume was too high, the compact configuration would have been chosen.

Lastly, the restrictive elements of additive manufacturing must be investigated. For voxelization, each dimension is converted from mm to voxels. For material jetting, this conversion rate is based on the printer's dots-per-inch and layer height. For the sake of this example, 299.73 dpi and 0.01875 mm, respectively, were used. The minimum feature size was estimated to be 1 voxel (approx. 0.085 mm). The required spacing panels, which was based on the membrane thickness, did not violate these restrictive elements. As an extra requirement, the authors required the geometry to be printed using material extrusion (MEX). The purpose was to validate the geometric functionality of the design. This increased the minimum feature size to twice the nozzle diameter[52] used to print Figures 4b and c (0.8 mm) and the Z minimum feature size of 1 layer, or 0.18 mm. Despite this constraint, the part successfully passes the minimum feature size requirements within the framework. Lastly, the small scale of the part meant it fit within the dimensions of most prints, meaning the geometry or printer did not need to be altered. Given that the part did not require alterations, no iterations were needed to produce this part.

### 4.2. Offset Panels TAM

This second case study also uses the framework provided in Figure 3. For the purposes of brevity, this section mentions variables and considerations that differ from the previous case study.

#### 4.2.1 Geometric Considerations of the Offset Panels TAM

The geometry for the Offset Panels TAM is listed in Table 4 with annotations in Figure 5. As in the previous case study, this TAM was made using a planar mechanism. Unlike the previous case study, this TAM requires an AM-adapted fold. This fold intersects two panels and has a slight curve. The intersection is loosely based on Ye et al.'s findings that surrounding a material with another material can prevent delamination [34]. The curve was added to prevent the interface from perfectly aligning with either axis when printed and to increase length of the fold, when compared to a straight line. One non-biasing cutout was used, to separate the AM-adapted fold into two folds; one coincident with the top of the part and one coincident with the bottom of the part.

#### 4.2.2 Material Considerations of the Offset Panels TAM

Following the framework in Figure 3, two gradients were used per AM-adapted fold. A two-dimensional gradient in the "X" and "Y" directions was used because the AM-adapted fold was not symmetric; more flexibility was needed along one direction as opposed to the other. The Offset Panels TAM requires bending at the very edge of the panels. The region where these edges meet is approximately 1 voxel wide. A radial margin of 2 voxels was added to supplement the small region. A fully-rigid circle with a radius of 5 voxels is in the center of the AM-adapted fold for this reason. An ellipse was used because the AM-adapted folds are longer in one direction. The axes of the ellipse were 19 voxels and 89 voxels. The circle was made concentric to the elliptical gradient.

For the gradient rate of change, the linear relationship was still assumed; however, the "exp" value of "1" was chosen to provide an example of a truly linear gradient. The approximated trend

| Dimension | Dimension Abbreviation | Value (mm) |
|---|---|---|
| Panel Thickness | $t_P$ | 10 |
| Spacing | $S_P$ | 0.8 |
| Panel 1 Length | $L_{P1}$ | 50 |
| Panel 1 Width | $w_{P1} = w_{P1a} + w_{P1b} + S_P$ | 30.8 |
| Panel 2 Length | $L_{P2}$ | 34.2 |
| Panel 2 Width | $w_{P2} = w_{P1a}$ | 15 |
| Border | B | 2 |
| AM -adapted Fold Outer Radius | $R_O$ | 11.5 |
| AM-adapted Fold Inner Radius | $R_I$ | 10.5 |
| Fold Length | $L_F$ | 3.78 |
| Non-biasing Cutout Distance | $C_{NBD}$ | 6 |
| AM-adapted Fold Thickness | $t_F$ | 2 |

**Table 4:** Dimensions used in Case Study 2. Due to symmetry, the dimensions for two of the four panels are provided

line was similar to the example provided in the case study; however, the normalized term formula was altered to subtract the area of the circle, which was already accounted for. Once again, the full property range of the theoretical materials were used. Everything inside the circle was programmed to be fully flexible in MATLAB; everything outside of the ellipse was programmed to be fully rigid in MATLAB. This concludes the material considerations for the Offset Panels TAM. The voxelized part can be found in Figure 5a.

### 4.2.3 Printing Considerations of the Offset Panels TAM

As in the previous case study, this part was printed in the XY orientation primarily based on the loading condition of the part and secondarily based on the support material. Next in the framework is the printing configuration. This part was printed in the compact configuration because support material could be avoided when printed in the XY orientation and because printing in the expanded configuration would drastically increase the computational volume. Next, restrictive elements of AM were evaluated. The main consideration for this part was the spacing between panels. This required a gap no less than twice nozzle diameter to account for the minimum feature size [52]. As in the previous case study, the limiting factor was the minimum feature size of the material extrusion printer used to create the functional models in Figure 5b and d. Given that the original dimensions accounted for this, no iterations were needed. The bounding volume of the part was 50 mm x 62 mm x 10 mm, which fits within the volume of most desktop material extrusion printers.

## 5. Conclusion

This paper provides a framework for designing and manufacturing multi-material additively manufactured origami-based designs. This framework enables a user to select a thickness accommodation method based on the advantage AM adoption will bring to the TAM. Considerations such as geometry-, material-, and printing-related variables were demonstrated using two case studies. Voxel-based design was used to create a conceptual model. The first case study used a membrane TAM and involved a 1D gradient; the second case used offset panels and a 2D gradient.

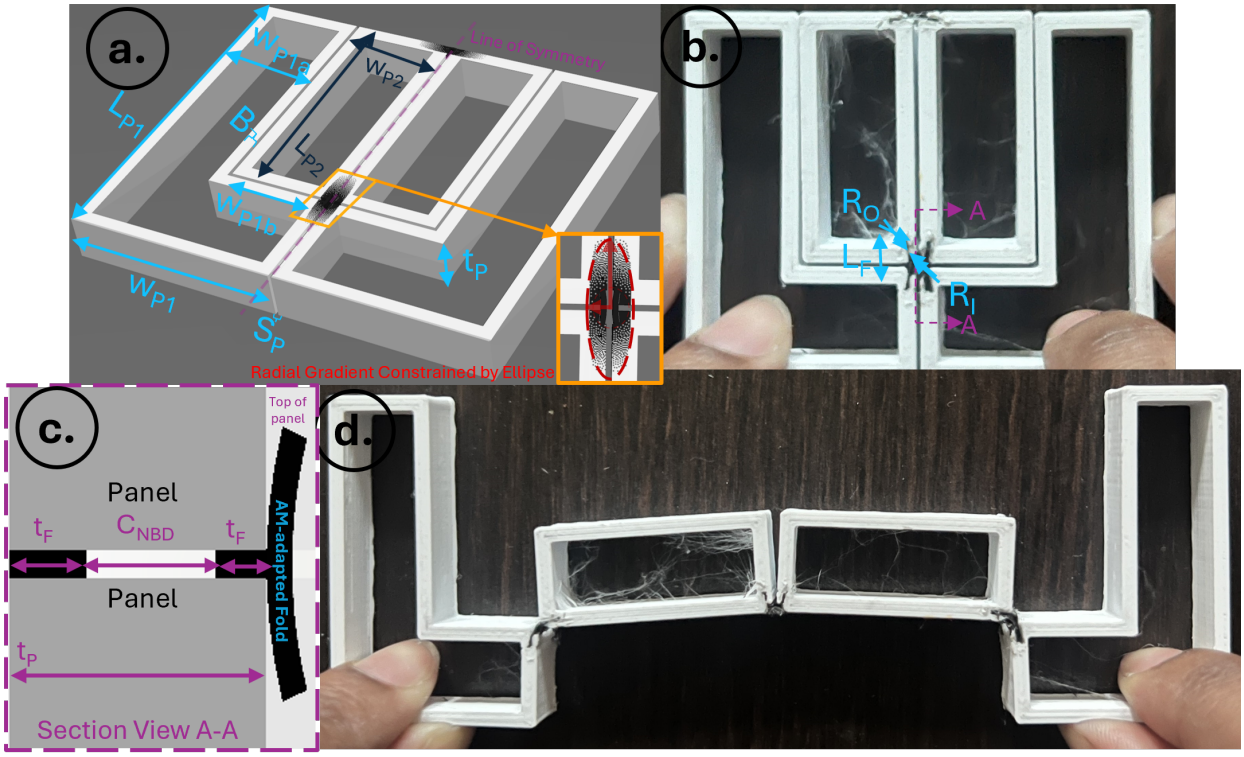


**Figure 5:** Case Study 2: The Offset Panels TAM. (a) Dimensioned Model (b) Voxel-based design (c) Section view of AM-adapted Fold (d) Unfolded Planar Model (MEX)

Although this work takes strides to guide users in applying voxel-based design to origami-based systems, some improvements can be made. This framework provides a non-exhaustive list of variables that can be used to design and manufacture these parts. Additional design guidelines such as performance considerations will be investigated. For example, information that checks if a part will yield or fail when folded. Yielding is not unusual for large-displacement, plastic parts; however, this could be detrimental if it does not meet the user's needs. Determining if the maximum stress within the part is lower than the ultimate stress or yield stress would provide more information to the user about how the part may perform when loaded. Another improvement includes more validation. The geometric considerations have been validated using the MEX models for the case studies provided; however, the material considerations must be validated using material jetting. Secondly, the scope of the case studies was limited to planar mechanisms. The next logical extension will be to demonstrate this framework using a foldable origami vertex. Lastly, introducing more opportunistic additive manufacturing considerations to this framework will further enhance the efficiency of the part. This was subtly shown by the border in Case Study 2; however, implementing this into the framework will ensure this step is not overlooked during the design process.

## 6. Acknowledgement

The first author was supported by the Department of Defense (DoD) through the National Defense Science & Engineering Graduate (NDSEG) Fellowship Program.

## References


[1] Jessica Morgan, Spencer P. Magleby, and Larry L. Howell. An Approach to Designing Origami-Adapted Aerospace Mechanisms. *Journal of Mechanical Design*, 138(5):052301, 03 2016.

[2] Bryce J. Edmondson, Landen A. Bowen, Clayton L. Grames, Spencer P. Magleby, Larry L. Howell, and Terri C. Bateman. Oriceps: Origami-Inspired Forceps. volume Volume 1: Development and Characterization of Multifunctional Materials; Modeling, Simulation and Control of Adaptive Systems; Integrated System Design and Implementation of *Smart Materials, Adaptive Structures and Intelligent Systems*, page V001T01A027, 09 2013.

[3] Jared Butler, Jessica Morgan, Nathan Pehrson, Kyler Tolman, Terri Bateman, Spencer P. Magleby, and Larry L. Howell. Highly Compressible Origami Bellows for Harsh Environments. volume Volume 5B: 40th Mechanisms and Robotics Conference of *International Design Engineering Technical Conferences and Computers and Information in Engineering Conference*, page V05BT07A001, 08 2016.

[4] Daniela Rus and Michael T. Tolley. Design, fabrication and control of origami robots. *Nature Reviews Materials*, 3(6):101–112, Jun 2018.

[5] S. Felton, M. Tolley, E. Demaine, D. Rus, and R. Wood. A method for building self-folding machines. *Science*, 345(6197):644–646, 2014.

[6] Junfeng Hu, Hu Li, and Weilong Chen. A squid-inspired swimming robot using folding of origami. *The Journal of Engineering*, 2021(10):630–639, 2021.

[7] Benjamin V. Johnson, Zekun Gong, Brian A. Cole, and David J. Cappelleri. Design of Disposable 3D Printed Surgical End-Effectors for Robotic Lumbar Discectomy Procedures. volume Volume 5A: 42nd Mechanisms and Robotics Conference of *International Design Engineering Technical Conferences and Computers and Information in Engineering Conference*, page V05AT07A055, 08 2018.

[8] Yan Chen, Rui Peng, and Zhong You. Origami of thick panels. *Science*, 349(6246):396–400, 2015.

[9] Yi Zhu and Evgueni T. Filipov. Large-scale modular and uniformly thick origami-inspired adaptable and load-carrying structures. *Nature Communications*, 15(1):2353, Mar 2024.

[10] Jared Butler, Nathan Pehrson, and Spencer Magleby. Folding of Thick Origami Through Regionally Sandwiched Compliant Sheets. *Journal of Mechanisms and Robotics*, 12(1):011019, 10 2019.

[11] Meredith Johnson, Yue Chen, Sierra Hovet, Sheng Xu, Bradford Wood, Hongliang Ren, Junichi Tokuda, and Zion Tsz Ho Tse. Fabricating biomedical origami: a state-of-the-art review. 12(11):2023–2032.

[12] Kirsten Lussenburg, Aimée Sakes, and Paul Breedveld. Design of non-assembly mechanisms: A state-of-the-art review. *Additive Manufacturing*, 39:101846, 2021.

[13] Jovana Jovanova, Simona Domazetovska, and Mary Frecker. Modeling of the Interface of Functionally Graded Superelastic Zones in Compliant Deployable Structures. volume Volume 2: Mechanics and Behavior of Active Materials; Structural Health Monitoring; Bioinspired Smart Materials and Systems; Energy Harvesting; Emerging Technologies of *Smart*

*Materials, Adaptive Structures and Intelligent Systems*, page V002T06A013, 09 2018.

[14] Dorcas V. Kaweesa and Nicholas A. Meisel. Quantifying fatigue property changes in material jetted parts due to functionally graded material interface design. *Additive Manufacturing*, 21:141–149, 2018.

[15] Robert J. Lang, Kyler A. Tolman, Erica B. Crampton, Spencer P. Magleby, and Larry L. Howell. A Review of Thickness-Accommodation Techniques in Origami-Inspired Engineering. *Applied Mechanics Reviews*, 70(1):010805, 02 2018.

[16] Fatemeh Zabihi and Morteza Eslamian. Characteristics of thin films fabricated by spray coating on rough and permeable paper substrates. *Journal of Coatings Technology and Research*, 12(3):489–503, May 2015.

[17] O. F. Jensen and J. M. Hansen. Dimensional synthesis of spatial mechanisms and the problem of non-assembly. *Multibody System Dynamics*, 15(2):107–133, Mar 2006.

[18] Arthur Erdman and Malachi Lehman. A Review of Kinematic Theories and Practices Compiled for Biomechanics Students and Researchers. *Journal of Biomechanical Engineering*, 146(5):050801, 03 2024.

[19] Michael Rider. *Design and Analysis of Planar Mechanisms*. 05 2015.

[20] Ziming Chen, Xuechan Chen, Min Gao, Chen Zhao, Kun Zhao, and Yanwen Li. Motion characteristics analysis of a novel spherical two-degree-of-freedom parallel mechanism. *Chinese Journal of Mechanical Engineering*, 35(1):29, Apr 2022.

[21] Alden Yellowhorse, Robert J. Lang, Kyler Tolman, and Larry L. Howell. Creating linkage permutations to prevent self-intersection and enable deployable networks of thick-origami. *Scientific Reports*, 8(1):12936, Aug 2018.

[22] Yuta Shimoda, Tomohiro Tachi, and Jun Sato. Pan. *Advances in Architectural Geometry*, pages 196–215, 2020.

[23] Tomohiro Tachi. Rigid-foldable thick origami. 5, 06 2011.

[24] D. Deng and Y. Chen. Assembled additive manufacturing - a hybrid fabrication process inspired by origami design. *24th International SFF Symposium - An Additive Manufacturing Conference, SFF 2013*, pages 174–187, 01 2013.

[25] Bingcong Jian, Frédéric Demoly, Yicha Zhang, and Samuel Gomes. An origami-based design approach to self-reconfigurable structures using 4d printing technology. *Procedia CIRP*, 84:159–164, 2019. 29th CIRP Design Conference 2019, 08-10 May 2019, Póvoa de Varzim, Portgal.

[26] Sang-Hun Kim, Hyunki In, Jeong-Ryul Song, and Kyu-Jin Cho. Force characteristics of rolling contact joint for compact structure. In *2016 6th IEEE International Conference on Biomedical Robotics and Biomechatronics (BioRob)*, pages 1207–1212, 2016.

[27] Jean-Michel Boisclair, Thierry Laliberté, and Clément Gosselin. On the Design of an Adaptable Underactuated Hand Using Rolling Contact Joints and an Articulated Palm. *Journal of Mechanisms and Robotics*, 15(5):051001, 11 2022.

[28] Shahram Janbaz, Niels Noordzij, Dwisetya S. Widyaratih, Cornelis W. Hagen, Lidy E. Fratila-Apachitei, and Amir A. Zadpoor. Origami lattices with free-form surface ornaments. *Science Advances*, 3(11):eaao1595, 2017.

[29] Weilin Lv, Wansui Nie, Jianjun Zhang, Yutong Wang, and Shijie Guo. Tapered Origami Tubes With Non-Planar Cross Sections. *Journal of Mechanisms and Robotics*, 16(7):074502, 11 2023.

[30] Kiju Lee, Yanzhou Wang, and Chuanqi Zheng. Twister hand: Underactuated robotic gripper

inspired by origami twisted tower. *IEEE Transactions on Robotics*, PP:1–13, 01 2020.
[31] Andreas Walker and Tino Stankovic. Algorithmic design of origami mechanisms and tessellations. *Communications Materials*, 3(1):4, Jan 2022.
[32] M. O. Barros, A. Walker, and T. Stanković. Computational design of an additively manufactured origami-based hand orthosis. volume 2, page 1231–1242, May 2022.
[33] Jakob A. Faber, Andres F. Arrieta, and André R. Studart. Bioinspired spring origami. *Science*, 359(6382):1386–1391, 2018.
[34] Haitao Ye, Qingjiang Liu, Jianxiang Cheng, Honggeng Li, Bingcong Jian, Rong Wang, Zechu Sun, Yang Lu, and Qi Ge. Multimaterial 3d printed self-locking thick-panel origami metamaterials. *Nature Communications*, 14(1):1607, Mar 2023.
[35] Isaac L. Delimont, Spencer P. Magleby, and Larry L. Howell. Evaluating Compliant Hinge Geometries for Origami-Inspired Mechanisms. *Journal of Mechanisms and Robotics*, 7(1):011009, 02 2015.
[36] Marius A. Wagner, Jian-Lin Huang, Philipp Okle, Jamie Paik, and Ralph Spolenak. Hinges for origami-inspired structures by multimaterial additive manufacturing. *Materials & Design*, 191:108643, 2020.
[37] Colin Hunter, Avinkrishnan Vijayachandran, and Anthony M. Waas. Self-deployable hinges for monolithic space structures using multi-material additive manufacturing. *Acta Astronautica*, 214:641–649, 2024.
[38] Peter A. Halverson, Larry L. Howell, and Spencer P. Magleby. Tension-based multi-stable compliant rolling-contact elements. *Mechanism and Machine Theory*, 45(2):147–156, 2010.
[39] Haitao Ye, Qingjiang Liu, Cheng Jianxiang, Honggeng Li, Bingcong Jian, Zechu Sun, and Qi Ge. Multimaterial 3d printed self-locking thick-panel origami metamaterials. *Nature Communications*, 14, 03 2023.
[40] Tsz-Ho Kwok. Geometry-Based Thick Origami Simulation. *Journal of Mechanical Design*, 143(6):061701, 11 2020.
[41] Jinho Woo and Won-Bae Na. Effect of cutout orientation on stress concentration of perforated plates with various cutouts and bluntness. *International Journal of Ocean System Engineering*, 1(2):95–101, 06 2011.
[42] Antonio J. Rubio, Abdul-Sattar Kaddour, Hunter T. Pruett, Larry L. Howell, Spencer P. Magleby, and Stavros V. Georgakopoulos. Volume-efficient miura-ori reflectarray antenna for smallsat applications. In *2022 IEEE International Symposium on Antennas and Propagation and USNC-URSI Radio Science Meeting (AP-S/URSI)*, pages 169–170, 2022.
[43] Evelyn Thomas, Nicholas Meisel, and Jared Butler. A Framework Establishing the Bounds of Small Angle Assumptions in Multi-Material Additively Manufactured Compliant Mechanisms. volume Volume 3A: 49th Design Automation Conference (DAC) of *International Design Engineering Technical Conferences and Computers and Information in Engineering Conference*, page V03AT03A044, 08 2023.
[44] Guimin Chen, Spencer P. Magleby, and Larry L. Howell. Membrane-Enhanced Lamina Emergent Torsional Joints for Surrogate Folds. *Journal of Mechanical Design*, 140(6):062303, 04 2018.
[45] Robert J. Lang, Todd Nelson, Spencer Magleby, and Larry Howell. Thick Rigidly Foldable Origami Mechanisms Based on Synchronized Offset Rolling Contact Elements. *Journal of Mechanisms and Robotics*, 9(2):021013, 03 2017.
[46] Jason S Ku and Erik D Demaine. Rigid folding analysis of offset crease thick folding. In

*Proceedings of IASS Annual Symposia*, volume 2016, pages 1–8. International Association for Shell and Spatial Structures (IASS), 2016.

[47] Brant Stoner, Joseph Bartolai, Dorcas V. Kaweesa, Nicholas A. Meisel, and Timothy W. Simpson. Achieving functionally graded material composition through bicontinuous mesostructural geometry in material extrusion additive manufacturing. *JOM*, 70(3):413–418, 2017.

[48] Sang-Joon Ahn, Howon Lee, and Kyu-Jin Cho. 3d printing with a 3d printed digital material filament for programming functional gradients. *Nature Communications*, 15(1):3605, May 2024.

[49] Alireza Fallahi Arezoodar and Ali Baladi. The effects of materials properties angle junction on stress concentration at interface of dissimilar materials. *Advanced Materials Research-Manufacturing Science and Technology*, Vols. 383-390 (2012):pp 887–892, 01 2012.

[50] Andrey Yu. Fedorov and Valerii P. Matveenko. Designing of interlayers between materials with minimum stress level at the interface. *International Journal of Adhesion and Adhesives*, 111:102963, 2021.

[51] Tobias Maconachie, Martin Leary, Jianjun Zhang, Alexander Medvedev, Avik Sarker, Dong Ruan, Guoxing Lu, Omar Faruque, and Milan Brandt. Effect of build orientation on the quasi-static and dynamic response of slm alsi10mg. *Materials Science and Engineering: A*, 788:139445, 2020.

[52] Simon J. Leigh. Using large-scale additive manufacturing as a bridge manufacturing process in response to shortages in personal protective equipment during the covid-19 outbreak. *IJB*, 6(4):281.